Features of Spectral-Angular Distribution of Coherent X-Radiation

V. B. Gavrikov[1], V. P. Likhachev[2], M. N. Martins[2], and V. A. Romanov[1]

[1] *Kharkov Institute of Physics and Technology, 310108 Kharkov, Ukraine*

[2] *Instituto de Física da Universidade de São Paulo,*

Laboratório do Acelerador Linear

Caixa Postal 66318, 05315-970, São Paulo, SP, Brasil

Received 10 May, 1999

The properties of coherent X-radiation (CXR), generated in crystals by electrons in the tens of MeV energy range, were investigated theoretically. The analytical expressions for CXR spectral-angular and angular cross sections were obtained with the use of small-angle multiple scattering approximation. Our theoretical results are in good agreement with experiment. The obtained results can be used in designing quasi-monochromatic, tunable and polarized X-radiation sources based on the CXR process.

I Introduction

Electromagnetic radiation produced in the interaction of a charged particle with an atomic system is the oldest and most traditional subject of quantum electrodynamics. Nevertheless, for a long time atomic electrons were not considered as a dynamic system and their role in the bremsstrahlung process was confined to screening the nuclear charge [1]. The reaction of the atomic electrons to the field of the incoming particle was treated either by Weizsäcker-Williams [2] or by classical electrodynamics methods [3]. The complexity of an integral description of the interaction process was clearly formulated by Ter-Mikaelian [2] in 1965: "Besides of nuclear bremsstrahlung it is necessary to take into account a radiation that is generated by atomic electrons. This question, with taking into account a binding of atomic electrons, is not considered yet by the accurate methods of the quantum electrodynamics".

The problem has been thoroughly investigated in Refs. [4-7]. The bremsstrahlung amplitude is presented there as a sum of two terms, where one term results from polarization bremsstrahlung, defined by a dynamic polarization of the atom, and the other term comes from the static bremsstrahlung of the particle in the fields of the nucleus and atomic electrons.

In an amorphous medium the angular distributions of the radiation from polarization and static bremsstrahlung are well separated. The static bremsstrahlung is concentrated into a cone with an angle of the order of γ^{-1} (where γ is the Lorentz's factor of the incoming particle) around the direction of the incoming particle momentum. In contrast, polarization bremsstrahlung is weakly anisotropic and its shape does not depend on the energy of the incident particle.

When a relativistic particle interacts with a crystalline target the polarization bremsstrahlung angular distribution changes radically. In such medium the radiation kinematics allows only a discrete set of momentum transfers. As a result the polarization bremsstrahlung is practically directed along the so-called Bragg angles. Moreover, the probability of the process increases considerably in comparison with an amorphous medium, and the produced radiation presents a coherent character. We then call this kind of bremsstrahlung, which is induced by a relativistic charged particle in a crystal, as coherent X-ray radiation (CXR). The components of this radiation are the coherent static and coherent polarization bremsstrahlung. This last type of radiation is also called, in the current literature, as parametric X-radiation [8] or parametric X-radiation of type B [9].

Since the pioneering work at Tomsk [10], a large number of experiments have studied the CXR intensity and energy dependencies on the crystal orientation with respect to the incident beam axis. In particular,

at electron beam energies of the order of tens of MeV, experiments were carried out with crystals of silicon (at 25 MeV) [11,12], germanium (at 21 and 25.4 MeV) [13] and diamond (at energies below 10 MeV) [9]. The first reported observation of the interference effect between the polarization and static bremsstrahlung mechanisms of CXR was made in Ref. [14]. In Ref. [15] the shape and the orientation dependence of the CXR linewidth have been investigated experimentally and numerically, using Monte-Carlo simulation, for a germanium crystal and electron incident energy of 25.4 MeV; in Ref. [16] the linewidth of the radiation generated in a diamond crystal by 6.8 MeV electrons was determined experimentally applying an absorption technique.

The results of these investigations encouraged us to study theoretically the spectral-angular properties of CXR, under the assumption that the small-angle multiple scattering approximation is valid. Our results can be useful in designing quasimonochromatic, polarized and low-background X-ray sources that can be based on the CXR process.

II Coherent X-radiation cross section

A wide range of problems connected with the excitation of atomic bremsstrahlung by fast charged particles were treated in Refs. [4-7]. Radiation in the X-ray energy range can be conveniently treated using the form factor approximation and the appropriate spectral-angular cross section for coherent X-radiation that have been obtained in Refs. [17,18]. Consider the case of a relativistic particle having charge e_0, mass m_0, initial energy E and velocity $\vec{\nu}$, which interacts with a non-relativistic atom. As a result of this interaction a bremsstrahlung photon with wave vector $\vec{k}$, energy ω and polarization vector $\vec{e}_f$ is emitted into a solid angle $d\Omega$, around an angle θ. Assuming also that: (1) the crystal atoms do not change states during the interaction; (2) the inequality $\omega << E$ is satisfied for all relevant photon energies; and (3) the radiation energies are large compared to the electronic binding energies; then the cross section for this process can be written in the form:

$$\frac{d^3\sigma}{d\omega\, d\Omega} = \frac{1}{k}\sum_{\vec{g},\vec{e}_f}\sigma_0(\vec{g})\left(\frac{\vec{e}_f\cdot(k\vec{\beta}-\vec{g})}{2\vec{k}\cdot\vec{g}+g^2}-\frac{G(\vec{g})}{\gamma g^2}\frac{\vec{e}_f\cdot\vec{g}}{1-\vec{n}\cdot\vec{\beta}}\right)^2\delta(\omega-(\vec{k}+\vec{g})\cdot\vec{\nu}) \qquad (1)$$

where $\sigma_0(\vec{g}) = \frac{8\pi\alpha z^2 r_e^2}{a^3}F^2(\vec{g})S^2(\vec{g})e^{-g^2\langle u^2\rangle}$; $G(\vec{g}) = \frac{e_0 m}{e m_0}\frac{Z-F(\vec{g})}{F(\vec{g})}$; $\alpha = 1/137$; $\vec{\beta} = \vec{\nu}/c$; $z = e_0/e$; $\vec{n} = \vec{k}/k$; r_e is the classical radius of the electron; a is the lattice period; e and m are the charge and mass of the electron; function $S(\vec{g})$ is the structure factor; $F(\vec{g})$ is the atomic form factor and Z is the atomic charge; $\langle u^2\rangle$ is the mean-square displacement of the atoms from their equilibrium position, due to vibrations. The summation in Eq. (1) is over all the reciprocal lattice vectors $\vec{g}$ of the crystal and photon polarization directions. We have also used the following dispersion relation for bremsstrahlung photons: $\omega = kc$, where c is the speed of light.

The first term in the brackets of Eq. (1) describes the polarization bremsstrahlung, since it is defined by the dynamic polarization of the crystal atoms in the fields of the incoming particle and the bremsstrahlung photon. The second one describes the static (Bethe-Heitler) bremsstrahlung of the projectile in the common field produced by the nuclei and electrons of the crystal. The dependencies of the polarization and static amplitudes on the mass and charge of the incident particle are quite different. The static bremsstrahlung disappears as the incident particle mass tends to infinity, while the polarization term continues being non-zero. Obviously, a change in the sign of the charge of the incident particle results in a change of the sign of the interference term in the full bremsstrahlung cross section.

From Eq. (1) the connection between the bremsstrahlung photon energy and the relative orientation of vectors $\vec{k}$, $\vec{\nu}$ and $\vec{g}$ is given by

$$\omega = \frac{\vec{g}\cdot\vec{\nu}}{1-\vec{n}\cdot\vec{\beta}} \qquad (2)$$

Different reciprocal lattice vectors, $\vec{g}$, in Eq. (2), produce quite different photon energies, and so in the following we shall consider the bremsstrahlung cross section only for a specific vector $\vec{g}$.

To obtain an expression for the spectral-angular cross section, taking into account the multiple scattering process of the projectiles in a crystalline target volume, one needs to integrate Eq. (1) over the crystal thickness, t, and over the component of $\vec{\nu}$ perpendicular to the initial beam direction, $\vec{\nu_\perp}$, and write:

$$\left\langle \frac{d^3\sigma}{d\omega d\Omega} \right\rangle = \int d\vec{\nu}_\perp dt a^{-1} f(\vec{\nu}_\perp, t)\, \frac{d^3\sigma}{d\omega d\Omega} \qquad (3)$$

where $f(\vec{\nu}_\perp, t)$ is the distribution of $\vec{\nu}_\perp$ on the depth t of the target.

The scattering plane is defined as the plane passing through $\vec{k}$ and the initial beam direction, and in the following we shall use a coordinate system where the z-axis is directed along the initial beam direction, while the x-axis is parallel to and the y-axis normal to the scattering plane (Fig. 1). In the framework of the small-angle approximation of the multiple scattering theory [19], to be used throughout this paper, one can write $\nu_z = \nu$, $\nu_x = \xi\nu$, and $\nu_y = \eta\nu$, where ξ and η are used to indicate the track angles of the scattered particle, measured with respect to the initial beam direction (Fig. 1).

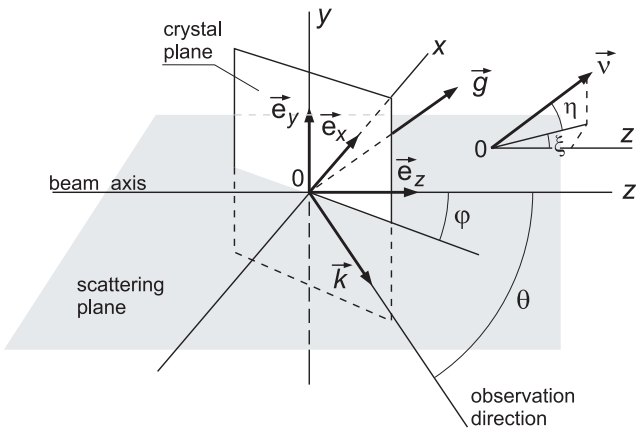

Figure 1. The coordinate system and definitions used in this paper. $\vec{k}$ is the wavevector of a bremsstrahlung photon; the particle beam is directed along the z-axis and θ is the observation angle; $\vec{e}_x, \vec{e}_y$ and $\vec{e}_z$ are unit vectors along the corresponding axes. The radiation is generated on a set of crystal planes, which are normal to the xz plane (scattering plane). Vector $\vec{g}$ lies in this plane and makes angle $\pi/2-\varphi$ with the z-axis. The angles ξ and η designate the track of a scattered particle.

A Gaussian distribution function will represent the distribution of relativistic particles after passing through a thickness t of the scattering material:

$$f(\vec{\nu}_\perp, t) = f(\xi,\eta,t) = \frac{1}{\pi\chi_c^2(t)\nu^2}\, e^{-(\xi^2+\eta^2)/\chi_c^2(t)} \qquad (4)$$

The function f is normalized according to:

$$\int_{-\infty}^{\infty} d\xi \int_{-\infty}^{\infty} d\eta\, f(\xi,\eta,t) = 1.$$

As in Ref. [19], the characteristic scattering angle, $\chi_c(t)$, for a homogeneous scatterer with no energy loss, is defined by:

$$\begin{aligned} \chi_c^2(t) &= \chi_0^2 t = 9\rho t Z(Z+1)/A\beta^4E^2 \text{ rad (for electrons)} \\ &= 9\rho t z^2 Z^2/A\beta^4E^2 \text{ rad (for heavy particles),} \end{aligned} \qquad (5)$$

where ρ is the density of the scatterer in g/cm^3, and A its atomic weight; E is given in MeV, and t in cm.

Summing over photon polarization directions in Eq.(1) and neglecting photon absorption, we obtain from Eq. (3) the spectral-angular cross section for CXR in the form:

$$\left\langle \frac{d^3\sigma}{d\omega d\Omega} \right\rangle = \frac{2\sqrt{\pi}}{\omega}\chi_0 \frac{L^{3/2}}{a} \frac{\sigma_0(\vec{g})}{[(\vec{k}+\vec{g})\cdot\vec{\beta}_x]}$$

$$\left\{ Q_1(p) \left[\frac{\vec{n} \times (k\vec{\beta}_z + k\theta_1\vec{\beta}_x - \vec{g})}{2\vec{k}\cdot\vec{g} + g^2} - \frac{G(\vec{g})}{\gamma g^2} \frac{\vec{n}\times\vec{g}}{[1 - \vec{n}\cdot(\vec{\beta}_z + \theta_1\vec{\beta}_x)]} \right]^2 + \frac{Q_2(p)}{6} \frac{(\vec{k}\times\vec{\beta}_y)^2}{(2\vec{k}\cdot\vec{g} + g^2)^2} \right\} \quad (6)$$

where L is the target thickness; $p = \beta^2\theta_1$; $\vec{\beta}_x = \beta\chi_0 L^{1/2}\vec{e}_x$; $\vec{\beta}_z = \beta\vec{e}_z$; $\vec{\beta}_y = \beta\chi_0 L^{1/2}\vec{e}_y$; and the functions Q_1 and Q_2 are defined by:
$Q_1(p) = e^{-p} - \sqrt{\pi p}(1 - erf(\sqrt{p}))$;
$Q_2(p) = e^{-p}(1-2p) + 2p\sqrt{\pi p}(1 - erf(\sqrt{p}))$,
and $\theta_1 = \frac{k - (\vec{k}+\vec{g})\cdot\vec{\beta}_z}{(\vec{k}+\vec{g})\cdot\vec{\beta}_x}$

In deriving Eq. (6) we neglected the terms which have order of $(\nu_\perp/\nu)^2$. In such approximation, fixed angles θ and φ determine the frequency with highest intensity. The linewidth can be estimated as $\theta_0 = \theta - 2\varphi$, the angular phase corresponding to the maximum frequency that can be observed at those angles or, in other words, the angular displacement that makes the intensity for that specific frequency go to zero. For this reason the calculations in Eq. (6) must be carried out up to the cutoff energy, defined by:

$$\omega_b = g\nu sin(\varphi + \theta_0)/(1 - \beta\cos(\theta + \theta_0)) \quad (7)$$

To calculate the intensity under the CXR peak, we must integrate Eq.(3) over ω , but the δ-function in Eq.(1) makes this integration straightforward. Defining the vector $\vec{k}_0 = \frac{\vec{n}(\vec{g}\cdot\vec{\beta}_z)}{1 - \vec{n}\cdot\vec{\beta}_z}$ and performing the integration in Eq.(3), we obtain the following expression for the coherent cross section:

$$\left\langle \frac{d^2\sigma}{d\Omega} \right\rangle = \frac{\pi\sigma_0(\vec{g})}{k_0} \frac{L}{a} \left\{ X_1^2 + \left(\frac{X_2}{1 - \vec{n}\cdot\vec{\beta}_z} \right)^2 - 2\frac{X_1 X_3}{1 - \vec{n}\cdot\vec{\beta}_z} + \chi_0^2 L Y^2 \right\} \quad (8)$$

where the functions
$X_1 = \vec{n} \times \left(\frac{k_0\vec{\beta}_z - \vec{g}}{2\vec{k}_0\cdot\vec{g} + g^2} - \frac{G(\vec{g})}{\gamma g^2} \frac{\vec{g}}{1 - \vec{n}\cdot\vec{\beta}_z} \right)$;

$X_2 = \vec{n} \cdot \left(\frac{(\vec{g}\cdot\vec{\beta}_x)\vec{\beta}_z + (\vec{g}\cdot\vec{\beta}_z)\vec{\beta}_x + (\vec{n}\cdot\vec{\beta}_x)\vec{g}}{2\vec{k}_0\cdot\vec{g} + g^2} - \frac{(k_0\vec{\beta}_z - \vec{g})[2(\vec{g}\cdot\vec{\beta}_x)(\vec{n}\cdot\vec{g}) - g^2\vec{n}\cdot\vec{\beta}_x]}{(2\vec{k}_0\cdot\vec{g} + g^2)^2} + \frac{G(\vec{g})}{\gamma g^2} \frac{\vec{g}(\vec{n}\cdot\vec{\beta}_x)}{1 - \vec{n}\cdot\vec{\beta}_z} \right)$;

$X_3 = \vec{n} \times \frac{[(\vec{g}\cdot\vec{\beta}_x)\vec{\beta}_z + (\vec{g}\cdot\vec{\beta}_z)\vec{\beta}_y + (\vec{n}\cdot\vec{\beta}_x)\vec{g}][2(\vec{g}\cdot\vec{\beta}_x)(\vec{n}\cdot\vec{g}) - g^2\vec{n}\cdot\vec{\beta}_x]}{(2\vec{k}_0\cdot\vec{g} + g^2)^2}$;

and $Y = \frac{k_0}{2\vec{k}_0\cdot\vec{g} + g^2}$.

Eqs. (6) and (8) have been obtained in the framework of the form factor approximation. Analysis of the limitations of this approximation in Ref. [20] shows that it is valid for $\omega \geq \omega_k$, where ω_k is K-shell ionization energy. Considering that the CXR intensity is concentrated in an angular interval $\varphi_{1,2} \approx \theta/2 \pm (2\gamma)^{-1}$, we found that the above formulas are suitable for the observation angles $\theta \geq \theta_0'$, where

$$\theta_0' = 3\frac{\omega_k}{\gamma g\nu} + 2\gamma^{-1} \quad (9)$$

For angles smaller than θ_0' it is necessary to take into account in Eq.(1) the spatial components of the transition currents of the atomic electrons [7].

III Results and discussion

The calculations were compared with the experimental results obtained at the Kharkov 40 MeV linear electron accelerator [21]. The accelerator provides 7 μs electron beam pulses at a repetition rate of 50 Hz with full an-

gle of divergence of about 1 mrad. The CXR spectra were produced in a 54(5)-μm thick germanium crystal on plane (220) and in a 30(3)-μm thick silicon crystal on plane (111) at different electron beam energies. The targets were mounted in a three-axis goniometer, allowing adjustment of the target with a resolution of 0.08 mrad.

The photon detector used in the measurements was a 5-mm thick Si(Li) solid-state detector, enclosed by a 25-μm Be window and placed directly into a vacuum photon channel oriented at an angle θ of 305.9 mrad with respect to the beam axis. The energy resolution of the detector was 350 eV (FWHM) for the 13.9 keV line of ^{241}Am. The solid angle subtended by the detector, was 4.49(5) $\times$ 10^{-7} sr. To avoid double counting in the detector, the coincidence gating was used and the beam current adjusted so that the total count rate did not exceed 0.2 counts per beam burst. The average beam current for this condition was 10^{-9} A. A more detailed description of the experimental setup and procedures can be found in Ref. [22].

All our calculations refer to a perfect crystal target at room temperature. The values of $F(\vec{g})$ used in the calculations were obtained from the data of Ref. [23]. For diamond-like crystals the value of $S(\vec{g})$ is equal to 64 for (220) planes and 32 for (111) planes.

In Fig. 2a we compare the measured and calculated shapes of the coherent X-radiation generated in the germanium target with beam energy of 25.4 MeV and at φ = 178 mrad. Figure 2b is analogous to Fig. 2a but for the silicon target, beam energy of 15 MeV, and φ = 128 mrad. The solid lines labeled 1 represent the calculations of the spectral density obtained using Eq. (6). The lines labeled 2 show the spectral density resulting from the convolution of lines 1 with the energy resolution function of the detector.

The measured and calculated orientation dependences of the CXR linewidth, that are understood as the second moment of the corresponding spectral density distributions, are shown in Fig. 3 for the germanium target and beam energy of 25.4 MeV. The solid and dashed lines represent the calculations of Eq. (6), respectively accounting and not for the detector resolution.

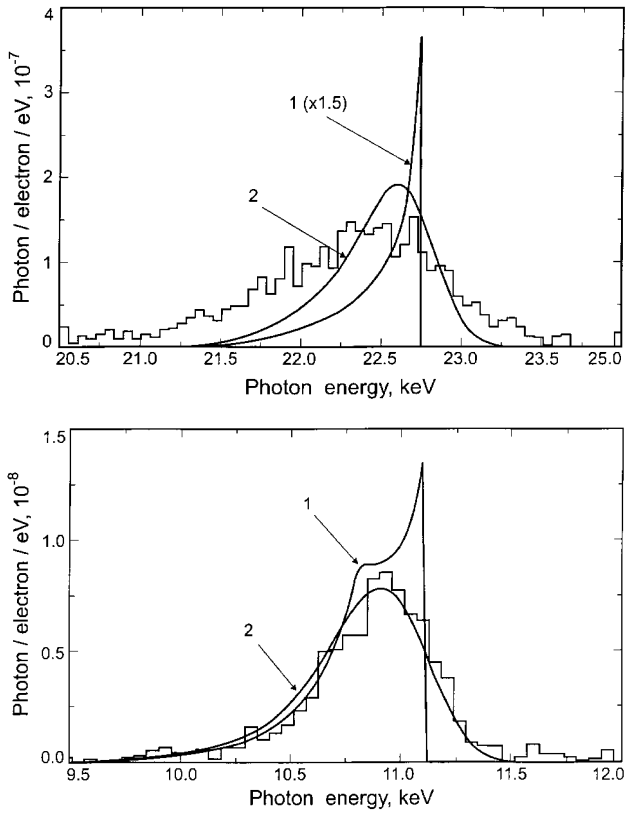

Figure 2. The observed and calculated spectral density of coherent X-radiation for (a) the germanium crystal (beam energy 25.4 MeV, φ = 178 mrad) and (b) for the silicon crystal (beam energy 15 MeV, φ = 128 mrad). The solid lines labeled 1 represent the calculation of the spectral density obtained using Eq.(6). The lines labeled 2 show the spectral density resulting from the convolution of lines 1 with the energy resolution function of the detector. Note that in these spectra background has been subtracted.

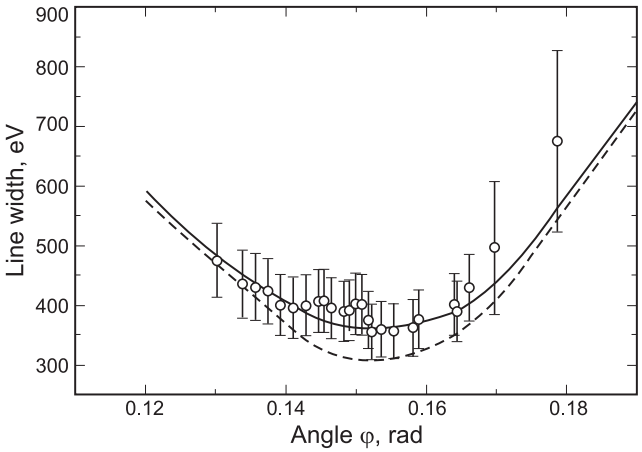

Figure 3. The observed and calculated dependences of the linewidths of the radiation induced by 25.4 MeV electrons in the germanium crystal. The solid and dashed lines represent the calculations of Eq.(6), respectively accounting and not for the detector resolution.

There are several reasons for the line broadening of atomic bremsstrahlung. The expression for the coher-

ent cross section, Eq. (1), has a δ-function which results from the product of terms like $\frac{sin^2(N_i\vec{a}_i\cdot\vec{q}/2)}{sin^2(\vec{a}_i\cdot\vec{q}/2)}$ [24], where $i = x, y, z$; $\vec{a}_i$ are the primitive lattice vectors; N_i the number of primitive unit cells along the ith edge of the crystal and $\vec{q}$ is the momentum transfer, at $N_i \to \infty$. For a crystal of finite thickness, which has N_z unit cells along the beam axis, one can estimate that the radiation line will be spread around the center by

$$\delta\omega \approx \omega N_z^{-1} \tag{10}$$

where ω is given by Eq. (2). For the crystals under consideration $\delta\omega$ is about 0.2 eV.

Another type of line broadening is associated with a finite solid angle acceptance of the detector. According to Eq. (2) the line spread is given by:

$$\delta\omega \approx \omega \sin\theta\Delta\theta/(1-\beta\cos\theta)^2 \tag{11}$$

where $\Delta\theta$ is the angular size of the detector opening. For our experimental conditions Eq. (11) gives about 25 eV for the silicon target and 50 eV for the germanium one.

Other contributions to the linewidth, associated with crystal imperfections, energy spread and angular divergence of the incident beam, or with a small misalignment of the detector, may be evaluated with formulas like Eq. (11).

But the main contribution to the radiation linewidth arises from multiple scattering. Analysis of Eq. (6) shows that the minimum value of the linewidth is achieved at

$$\varphi_{\min} \approx \frac{\theta^2 + \chi_0^2 L}{2\theta} \tag{12}$$

and the corresponding line spread is

$$\delta\omega \approx \frac{g\nu\chi_0^2 L}{\theta(\theta^2 - \chi_0^2 L)} \tag{13}$$

Using Eq. (13) one can find $\delta\omega = 146$ eV ($\omega = 12.6$ keV) for the silicon crystal and beam energy of 15 MeV, and $\delta\omega = 420$ eV ($\omega = 19.8$ keV) for the germanium crystal and a 25.4 MeV beam.

Figure 4 shows the measured and calculated CXR intensity dependence on orientation for the silicon crystal and beam energy of 25 MeV. The solid line presents the calculated dependence following from Eq.(8), and the dashed line the dependence calculated without multiple scattering. The indicated experimental errors include both statistical errors and errors due to the charge measuring procedure.

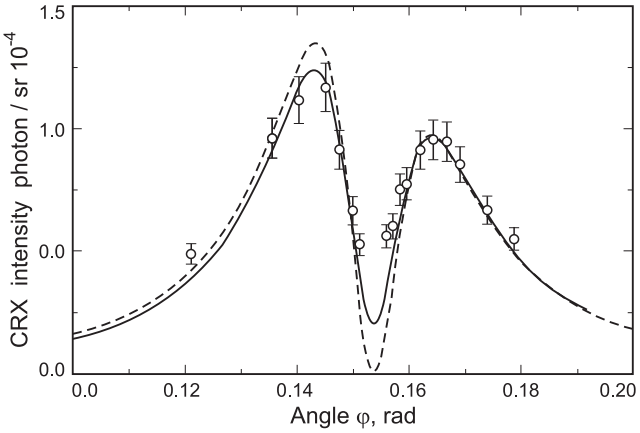

Figure 4. The orientation dependence of the CXR intensity on the angle φ. The experimental points have been obtained for the silicon crystal at beam energy of 25 MeV. The calculation has been carried out using Eq. (8). The dependence without taking into account multiple scattering is shown by the dashed line.

Equation (8) gives a clear physical picture of the coherent radiation process. The first term in the curly brackets of Eq. (8) describes the process without taking into account multiple scattering; the other terms are responsible for changing the radiation characteristics due to multiple scattering. Neglecting multiple scattering, the cross section presents a zero at:

$$\varphi_0 = \frac{\theta}{2}\left[1 + \frac{1}{\gamma^2\theta^2} + \frac{G(\vec{g})}{\gamma^3\theta^4}\right] \tag{14}$$

and maxima at:

$$\varphi_{\max} \approx \theta/2 \pm 1/2\gamma \tag{15}$$

The angular dependence of the cross section at the maxima given by Eq. (15) is

$$\left\langle \frac{d^2\sigma}{d\Omega} \right\rangle_{\max} \propto (1 \mp \gamma\theta)^2 \tag{16}$$

In Eq. (8) the multiple scattering terms give negative contributions near the maxima, Eq. (15), and positive near the minimum at φ_0, Eq. 14 (see Fig. 4).

We can define two independent polarization directions, such that one (called σ-polarization) is parallel to and the other (π-polarization) is normal to the scattering plane. The terms containing functions X_1, X_2 and X_3, are associated with the σ-component, while function Y describes the π-component of the coherent radiation. It is clear that without multiple scattering the radiation is 100% linearly polarized.

IV Conclusions and outlook

One of the aims of our work is to show the potentialities of an X-ray source based on the CXR process. Obviously, such source presents interesting features: allows to obtain quasimonochromatic (Eqs. (10)-(13)), linearly polarized photons with tunable energy (Eq. (2)) and, moreover, almost free of background. The main drawback of such a source is its relatively low intensity. For typical operation conditions, the CXR source intensity loses a few orders of magnitude as compared to channeling [25] and synchrotron [26] radiation source intensities.

The characteristics of the CXR used for comparison were measured with extremely low electron beam currents (∼nA), limited by the count rate on the photon detector. This current corresponds to a photon flux (for a 5% energy resolution) of a few photons/mm^{2}s. On the other hand, X-ray intensities for most radiological applications are approximately between 10^9-10^{11} photons/mm^{2}s. To obtain such a flux, a much higher electron beam current is needed. Higher beam currents complicate the theoretical consideration, since it is necessary to take into account interference effects in the radiation, which may occur when several relativistic particles are inside a crystal volume simultaneously. So, as a first step of estimation (trivial), we can only extrapolate our pulsed current conditions (4 μs, 50 Hz) to a continuous wave operation, keeping the other parameters fixed. The cw current equal to our peak current (5 μA) corresponds to a photon flux of 10^6 photons/mm^{2}s (for a 5% bandwidth). To further increase the photon flux it would be necessary to increase either the crystal thickness or the cw current, which involve more complicated theoretical considerations.

The use of high beam currents rises also some technical problems, like crystal cooling and radiation damage. Experiments with crystals [27], show that a typical crystal withstands a beam current of 3-5 μA for thousands of hours. After that the crystal needs replacement.

Finally we can conclude that the main features of CXR (except for its maximum possible intensity) are well established, and it is necessary to find a field of application for this moderately intense source of quasimonochromatic and linearly polarized photons, practically free of bremsstrahlung background.

Acknowledgements

We thank Dr. V.L. Morokhovskii and Prof. A.A. Rukhadze for discussions of the involved problems. This work was supported by the State Committee of Science and Technology of Ukraine (Project Quanta) and, in part, by Grant UA3000 from the International Science Foundation.

References

[1] H. Olsen, L.C. Maximon, Phys. Rev. **114**, 887 (1959).

[2] M.L. Ter-Mikaelian, High-Energy Electromagnetic Processes in Condensed Media, Wiley-Interscience, New York, 1972.

[3] D. Dialetis, Phys. Rev. A **17**, 1113 (1978).

[4] M.Ya. Amusia, Comments Atom. and Mol. Phys. **11**, 123 (1982).

[5] M.Ya. Amusia, M.Yu. Kychiev, A.V. Korol, A.V. Soloviev, Sov. Phys. JETF, **88**, 383 (1985).

[6] V.A. Astapenko, V.M. Buymistrov, Yu.A. Krotov, Sov. Phys. JETF, **88**, 1560 (1985).

[7] M. Ya. Amusia, V.M. Buymistrov, B.A. Zon, V.N. Tsytovich, V. A. Astapenko, E.B. Kleiman, A.V. Korol, Yu.A. Krotov, A.B. Kukushkin, V.S. Lisitsa, I.N. Ostrynge, A.V. Soloviev, V.I. Kogan, Polarization bremsstrahlung of particles and atoms, Nauka, Moskow, 1987.

[8] H. Nitta, Phys. Rev. B **45**, N14, 7621 (1992).

[9] J. Freudenberger, V.B. Gavrikov, M. Galemann, H. Genz, L. Groening, V.L. Morokhovskii, V.V. Morokhovskii, U. Nething, A. Richter, J.P.F. Sellschop and N.F. Shul'ga, Phys. Rev. Lett. **74**, 2487 (1995).

[10] S.A. Vorob'ev, B.N. Kalinin, S. Pak, A.P. Potylitsyn, JETP Lett. **41**, 1 (1985).

[11] A.V. Shchagin, V.I. Pristupa, N.A. Khizhnyak, Phys. Lett. A **148**, 485 (1990).

[12] V.L. Morokhovskii, D.I. Adejishvili, V.B. Gavrikov, Ukrainian Phys. Jour. **38**, 389 (1993).

[13] D.I. Adejishvili, V.B. Gavrikov, V.L. Morokhovskii, Coherent scattering of relativistic electron field in Ge on (220) planes, in: Proc. of 24th Conf. on Physics of High-Energy Particle Interactions with Media, Moscow, 30 May - 1 June (1994) 58.

[14] S.V. Blazhevich, G.L. Bochek, V.B. Gavrikov, V.I. Kulibaba, N.I. Maslov, N.N. Nasonov, V.N. Pirogov, A.G. Safronov and A.V. Torgovkin, Phys. Lett. A **195**, 210 (1994).

[15] D.I. Adejishvili, V.B. Gavrikov, V.L. Morokhovskii, V.V. Morokhovskii, V.N. Pirogov, Linewidth of parametric X-radiation of type B measured in germanium at electron energy 25.4 MeV, Kharkov, KIPT 95-10 (1995)5p.

[16] J. Freudenberger, M. Galemann, H. Genz, L. Groening, P. Hoffmann-Stascheck, V.L. Morokhovskii, V.V. Morokhovskii, U. Nething, H. Prade, A. Richter, J.P.F. Sellschop and R. Zahn, Nucl. Instr. and Meth. B **115**, 408 (1996).

[17] D.I. Adejishvili, V.B. Gavrikov, V.L. Morokhovskii, About interference between parametric X-ray radiation of type B and coherent bremsstrahlung of fast charged particle in a crystal, Kharkov, KIFT 96-2 (1996) 9p.

[18] V.B. Gavrikov, Dissertation, Kharkov, Kharkov Institute of Physics and Technology, (1996).

[19] William T. Scott, Rev. Mod. Phys. **35**, 231 (1963).

[20] L. Kissel, R.H. Pratt, S.C. Roy, Phys. Rev. A **22**, 1970 (1980).

[21] D.I. Adejishvili, V.B. Gavrikov, V.A. Romanov, On the absolute intensity of parametric X-radiation, to be published in Nucl. Instrum. and Meth. B.

[22] D.I. Adejishvili, V.B. Gavrikov, I.F. Emel'yanchik, V.L. Morokhovskii, V.D. Ovchinnik, V.N. Pirogov, N.N. Hal'ko and D.S. Shvarkov, Program-apparatus complex for investigation of X- and gamma-rays generated by relativistic electrons in crystals, Kharkov, KIPT 91-8 (1991) 14p.

[23] J. Wang, R.P. Sagar, H. Schimider, V.H. Smith, Atomic Data and Nucl. Data Tables **53**, 233 (1993).

[24] A comprehensive description of coherent bremsstrahlung kinematics can be found in H. Uberall, Phys. Rev. **103**, 1055 (1956).

[25] W. Knupfer *et al.*, NIM B **87**, 98 (1994).

[26] W.R. Dix *et al.*, NIM A **314**, 307 (1992).

[27] V.P. Likhachev, M.N. Martins *et al.*, Nucl. Phys. A **628**, 597 (1998).